

Supporting Information

Self-focusing Au@SiO₂ nanorods with rhodamine 6G as highly sensitive SERS substrate for carcinoembryonic antigen detection

Tran Thi Bich Quyen^a, Chun-Chao Chang^{b,c}, Wei-Nien Su^d Yih-Huei Uen^{e,f,g}, Chun-Jern Pan^a, Jyong-Yue Liu^a, John Rick^a, Kai-Yuan Lin^{f,h}, , Bing-Joe Hwang^{a,i,*}

^aNanoelectrochemistry Laboratory, Department of Chemical Engineering, National Taiwan University of Science and Technology, Taipei 106, Taiwan

^bDivision of Gastroenterology and Hepatology, Department of Internal Medicine, Taipei Medical University Hospital, No. 250, Wu-Hsing St., Taipei 11031, Taiwan

^cDepartment of Internal Medicine, School of Medicine, College of Medicine, Taipei Medical University, No. 250, Wu-Hsing St., Taipei 11031, Taiwan

^dGraduate Institute of Applied Science and Technology, National Taiwan University of Science and Technology, Taipei 106, Taiwan

^eDivision of General Surgery, Department of Surgery, Chi Mei Medical Center, Tainan, 710, Taiwan

^fDepartment of Medical Research, Chi Mei Medical Center, Tainan, 710, Taiwan

^gInstitute of Biomedical Engineering, Southern Taiwan University of Science and Technology, Tainan, 710, Taiwan

^hDepartment of Biotechnology, Chia Nan University of Pharmacy and Science, Tainan, 717, Taiwan

ⁱNational Synchrotron Radiation Research Center, Hsinchu 30076, Taiwan

***Corresponding Authors:** Bing-Joe Hwang: Fax: +886-2-27376644; E-mail:bjh@mail.ntust.edu.tw;
National Taiwan University of Science and Technology

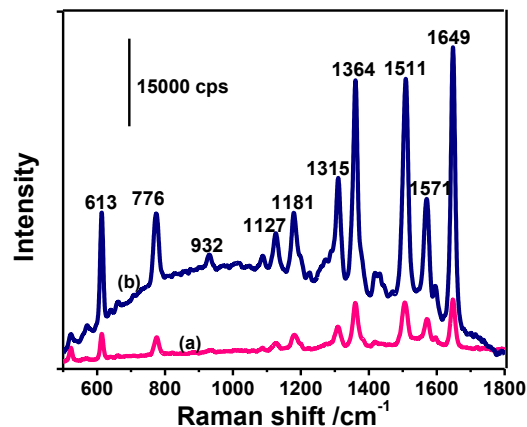


Fig. S1 Raman spectra of 10^{-8} M R6G on (a) Au@SiO₂ NPs (~40 nm core/ with shell 1-2 nm),¹ and (b) Au@SiO₂ NRs (~70 nm core/ with shell 1-2 nm), respectively.

The enhancement factors for SERS activity were calculated from the equation $EF = \frac{(I_{SERS}/C_{SERS})}{(I_{ref}/C_{ref})}$, taken from reference.² In this equation, C_{ref} (10^{-1} M) and C_{SERS} represent the concentrations of R6G on the silicon substrate and R6G on Au@SiO₂ NRs substrate used for obtaining the I_{ref} and I_{SERS} , respectively, in measurements.

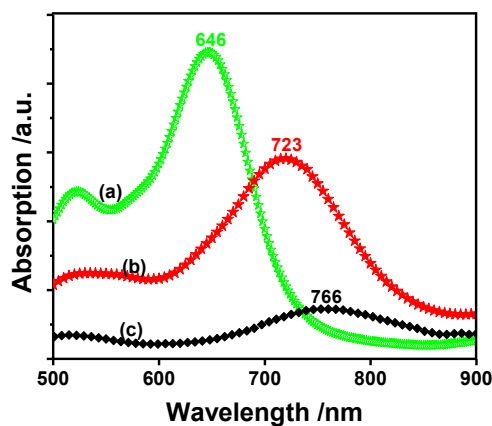


Fig. S2 UV-vis spectra of Au nanorods in different lengths: (a) 47 nm; (b) 70 nm; and (c) 82 nm

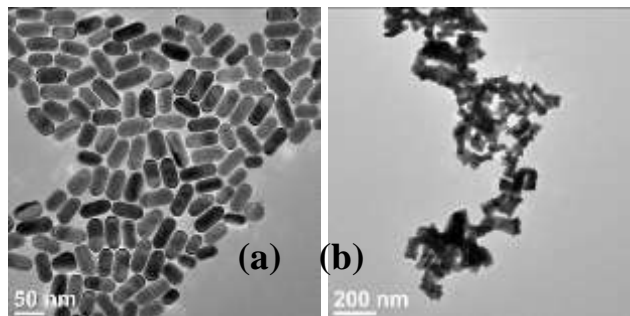


Fig. S3 TEM images of (a – b) Au nanorods (~47 nm, and ~82 nm with 15 μ L, and 8 μ L of Au seed solution), respectively.

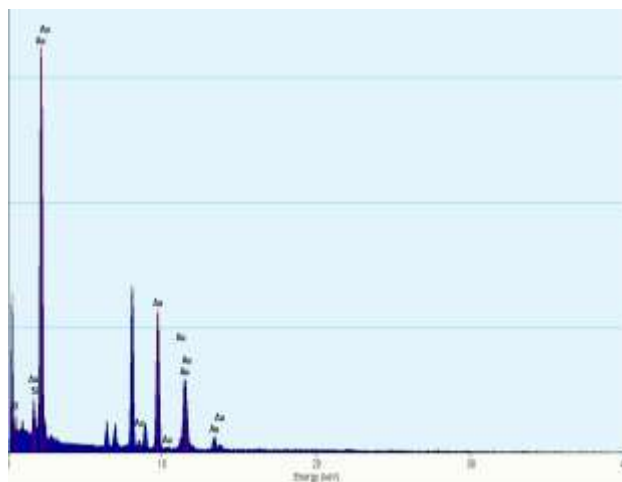


Fig. S4 EDX of Au@SiO₂ core/shell nanorods (~70 nm core/ with shell 1-2 nm)

Fig. S5 collects three sets of XRD patterns of Au NRs, and Au@SiO₂ NRs. In general, SiO₂ shows a broad amorphous feature at 2θ ($44^\circ - 77.74^\circ$) – see Fig. S5(b), and Au peaks appear at 2θ $38^\circ, 44^\circ, 65^\circ$, and 78° , corresponding to gold (111), (200), (220), and (311), respectively as shown in Fig. S5(a). These peaks are consistent with the Joint Committee on Powder Diffraction Standard (JCPDS 04-0784). The Au peaks become sharper with the growth of Au nanorods. On the other hand, SiO₂ maintains its amorphous phase, and the formation of new phases is not detected.

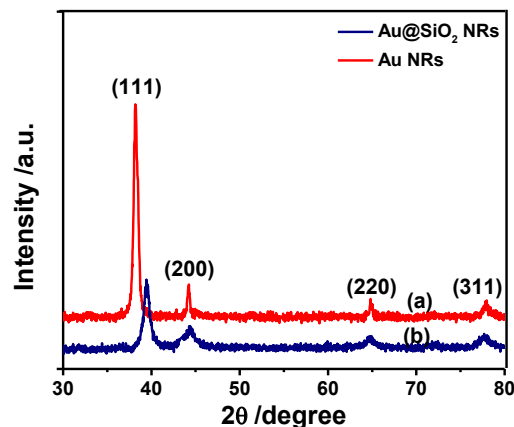


Fig. S5 XRD patterns of (a) Au NRs (~70 nm), and (b) Au@SiO₂ NRs (~70 nm core/ with shell 1-2 nm).

Fig. S6 shows SEM images of Au@SiO₂ NRs without CEA (before) and in the presence of CEA (after). Moreover, the inter-particle distances between two neighboring nanorods have been calculated to show how the CEA concentration significantly affects the SERS enhancement due to the “self-focusing” structure and different inter-particle distances. Fig. S7 shows the dependence of the self-focusing structure on the mean inter-particle distance and Raman intensity using Au@SiO₂ NRs (~70 nm core/ shell 1-2 nm) in the presence of various CEA antigen concentrations at 0 pg mL⁻¹, 1 pg mL⁻¹, and 100 pg mL⁻¹, respectively. When the CEA concentration increases, the distance between two particles becomes shorter, and the SERS signal intensity gets significantly higher. As shown in Fig. S8, the distribution of CEA antigens on Au@SiO₂ NRs carrying R6G and antibody (scan area: 20 × 20 μm²) is illustrated based on the highest signal intensity of peak at 1619 cm⁻¹. It should be noted that the uniform distribution of the R6G characteristic peak signals represented uniform CEA antigen-antibody distribution on the Au@SiO₂ NRs substrate in this wavenumber region can be attributed to the self-focusing structures that greatly enhanced the reliability of the measurements, as seen in the SERS mapping, Fig. S8.

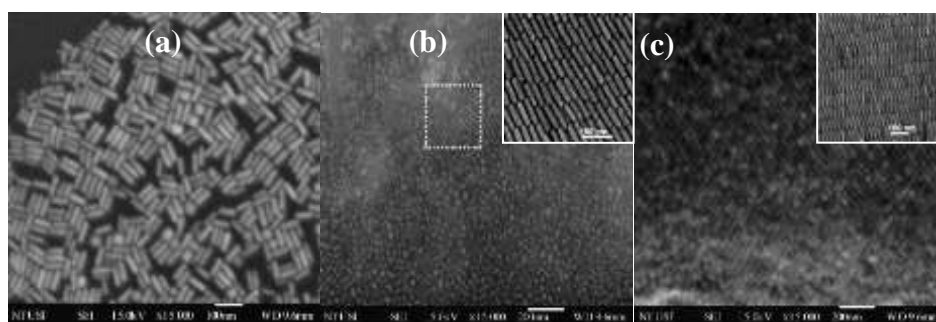


Fig. S6 SEM images of Au@SiO₂ NRs (~70 nm core/ shell 1-2 nm) in the presence of (a) 0 pg mL⁻¹, (b) 1 pg mL⁻¹ and (c) 100 pg mL⁻¹ CEA antigen concentration, and HRSEM images are also displayed as inserts, respectively.

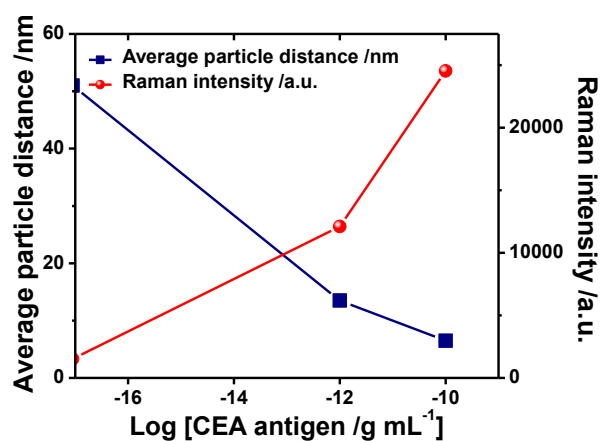


Fig. S7 Shows the self-assemble structure via the relative distance between particles and Raman intensity using Au@SiO₂ NRs substrate (~70 nm core/ shell 1-2 nm) in the presence of various CEA antigen concentrations at 0 pg mL⁻¹, 1 pg mL⁻¹, and 100 pg mL⁻¹, respectively. Each data point represents the mean value of ten distance measurements (i.e, the end-to-end distance between two particles) and average Raman intensity from three spectra.

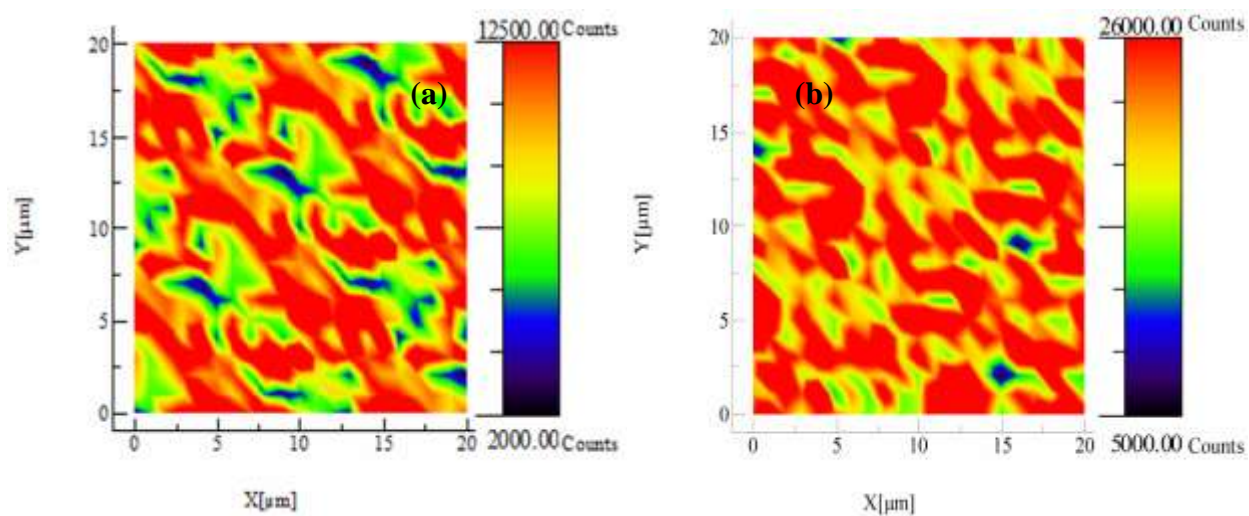


Fig. S8 SERS mapping of (a) 1 pg mL⁻¹ and (b) 100 pg mL⁻¹ CEA antigen on Au@SiO₂ NRs/R6G-conjugated with antibody after formation of self-focusing structures via the antibody-antigen interactions between Au@SiO₂ NRs based on signal of peak at 1619 cm⁻¹. This image is a 2D projection (scan area 20 \times 20 μm^2), respectively.

References

- 1 T. T. B. Quyen, W.-N. Su, K.-J. Chen, C.-J. Pan, J. Rick, C.-C. Chang and B.-J. Hwang, *J. Raman Spectrosc.* **2013**, DOI 10.1002/jrs.4400
- 2 E. C. Le Ru, E. Blackie, M. Meyer and P. G. Etchegoin, *J. Phys. Chem. C*, 2007, **111**, 13794-13803.